IEEE Access
Multidisciplinary | Rapid Review | Open Access Journal

Received August 11, 2018, accepted September 14, 2018, date of publication September 20, 2018, date of current version October 17, 2018.

Digital Object Identifier 10.1109/ACCESS.2018.2871462

Active Control of Pressure Resonance in Long Pipeline of Bottom Founded Hydraulic Wind Turbines Based on Multi-Objective Genetic Algorithm

CHAO AI[1,2], WENJIE BAI[2], TINGYUAN ZHANG[2], AND XIANGDONG KONG[1,2]
[1]Key Laboratory of Advanced Forging & Stamping Technology and Science, Ministry of Education of China, Yanshan University, Qinhuangdao 066004, China
[2]Hebei Heavy Machinery Fluid Power Transmission and Control Lab, Yanshan University, Qinhuangdao 066004, China

Corresponding author: Xiangdong Kong (xdkong@ysu.edu.cn)

This work was supported by the National Natural Science Foundation of China under Grant 51775476.

ABSTRACT The long pipeline in bottom-founded hydraulic wind turbines will greatly reduce the system natural frequency, and pressure resonances can occur more easily at multiple frequencies under time-varying wind excitation, which will reduce the electrical power quality and endanger the safe operation of the system. First, the hydraulic system impedance model is established based on electric–hydraulic analogy, and the pressure transfer function of two ends of the long pipeline is obtained, based on which the pressure resonance condition equation is solved by theoretical derivation. Furthermore, the multiple parameters sensitivity analysis of resonant frequency is carried out by using Isight and MATLAB. A novel active control strategy of pressure resonance is proposed, where the variable motor is adopted as the control object for real-time control of the terminal impedance to make the resonance frequency avoid the excitation frequency, and its feasibility is verified. Finally, with the objectives of optimizing the pressure pulsation attenuation and wind energy loss, a multi-objective genetic algorithm is used to optimize the parameters of the control object. A reliable Pareto set is obtained through multiple iterations, and different degrees of resonance suppression can be achieved.

INDEX TERMS Active control, hydraulic wind turbine, long pipeline, multi-objective genetic algorithm, pressure resonance.

I. INTRODUCTION

Many countries in the world are seeking renewable green energy to reduce environmental pollution, as a reliable, pollution-free and sustainable energy source, wind energy is increasingly favored. Various types of wind turbines are widely used in the utilization of wind energy, such as double fed induction generators (DFIG), direct-drive permanent magnet synchronous generators (D-PMSG) and so on. As a new type of wind turbine, hydraulic wind turbine adopts hydrostatic transmission system with compressible hydraulic oil as medium, compared with traditional wind turbines driven by gears, it not only has a higher power density, but also has a lower system stiffness, which can reduce the impact caused by the fluctuation of the wind and realize flexible transmission. In addition, gearboxes, inverters and transformers are eliminated, making the structure more compact. With the above advantages, hydraulic wind turbine is becoming research hotspots [1]–[5] for wind energy utilization and has extensive market application value.

Unlike most current configurations that place the entire hydraulic drive system in the nacelle as shown in Fig. 1a, bottom founded hydraulic wind turbines set the variable motor, synchronous generator and its corresponding control system at the base of the tower, the hydraulic transmission between the constant displacement pump at the nacelle and the variable motor at the tower base is realized by long pipelines fixed in the tower as shown in Fig. 1b. This configuration greatly reduces the nacelle weight and the difficulty of engineering installation [6].

In hydraulic systems, it is considered to be a long pipeline when the ratio of length to diameter is greater than 300, but for bottom founded hydraulic wind turbines with different

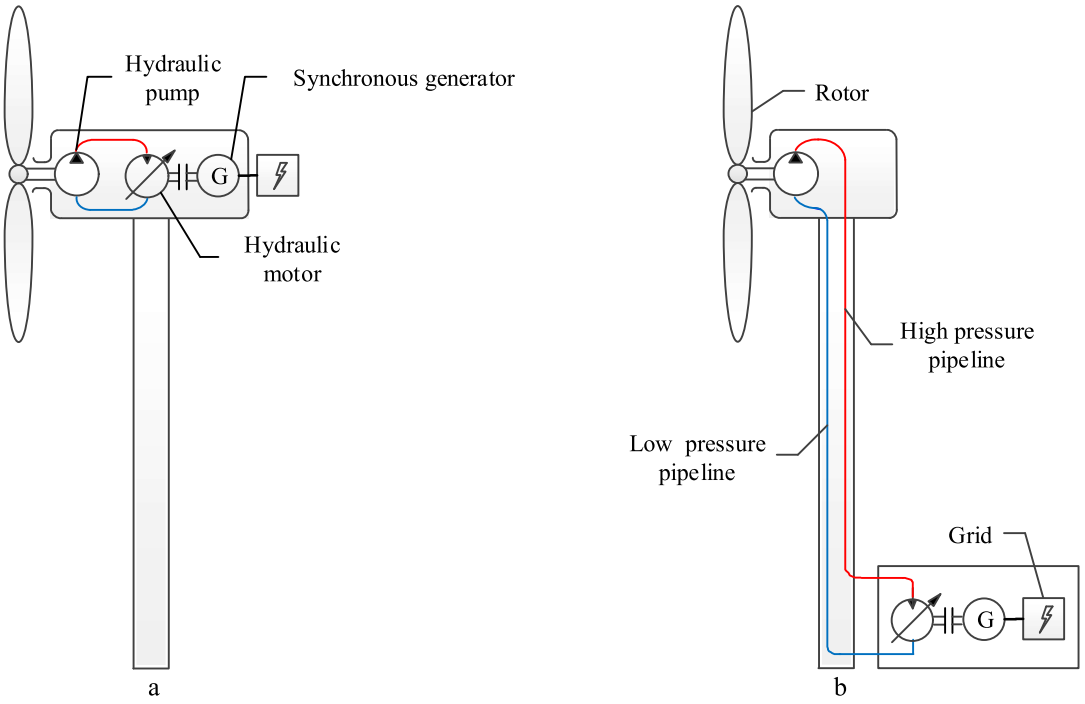

FIGURE 1. Hydraulic wind turbines with different configurations. (a) Nacelle solution. (b) Tower base solution.

power levels, the ratio is much greater than 300. Although the bottom founded hydraulic wind turbines have the aforementioned advantages, its long hydraulic pipelines will make the resonance effect more obvious, which can occur in a wide frequency range [7]. Besides, the output torque of the rotor which is excitation source of the hydraulic system has energy concentration at some time-varying frequency points when the wind is coupled with the deformation and vibration of the blades. Resonance occurs when the excitation frequency coincides with the resonance frequency. So a method is needed to reduce the potential strong pressure pulsation caused by long pipeline resonance.

In order to reduce pressure pulsation, a variety of passive pulsation attenuators are widely used in many occasions. However their application is limited because of its bad performance in low frequency area and lack of self-adaptability [8]. Therefore, more and more scholars have conducted in-depth research on active control of pressure pulsation, proposed many active control strategies using a plenty of control algorithms, and made some progress.

At present, the use of active control to reduce pressure pulsation mainly has three methods: the first way is to generate a pressure wave which is of equal amplitude but opposite polarity to the pulsating source. Jiao uses piezoelectric direct-drive slide valve as the control object [8], the rotating vector method [9] and gradient descent algorithm [10] are adopted to optimize the control parameters, experimental results show the amplitude of the pressure pulsation reduced by 63.3%. Pan adopts filtered-X least mean square algorithm for both in-series and by-pass structures of switched inertance hydraulic systems, and concludes that the by-pass structure can be more widely and effectively used for pulsation cancellation after comparison of the two structures in terms of system performance, robustness and advantages [11], then the controller is simplified with a rectangular-wave reference signal [12], experimental results show that an acceptable cancellation of 20dB can be achieved. The second method is to directly place non-intrusive actuators on the pipeline wall and counteract the pressure pulsation through the deformation of the pipeline wall. Jordan positioned an array of piezo stack actuators circumferentially around the pipe, the filtered-X LMS feedforward active control algorithm is adopted and a peak attenuation of around 30 dB is achieved experimentally [13]. Brennan designed a hydraulic actuator driven with a magnetostrictive element and arranged it on a water-filled perspex pipe, experimental results show that the actuator is capable of suppressing a propagating fluid-wave, significant reductions in dynamic pressure of between 30 and 40 dB were achieved over a wide frequency range [14]. The last method is to install servo actuators in the pipeline. Kojima [15], [16] designed a servo actuator as a secondary pulsation source, achieving a ripple attenuation effect of at least 20 dB.

The aforementioned scholars have made efforts on active control of pressure pulsation in the time domain and achieved significant results, a minimum amplitude attenuation of 20 dB and a maximum of 40 dB has been obtained using different methods. But all of current methods need to install extra devices in the system, which increases the structure complexity of the system. And the possible resonances at multiple frequency points caused by the distributed

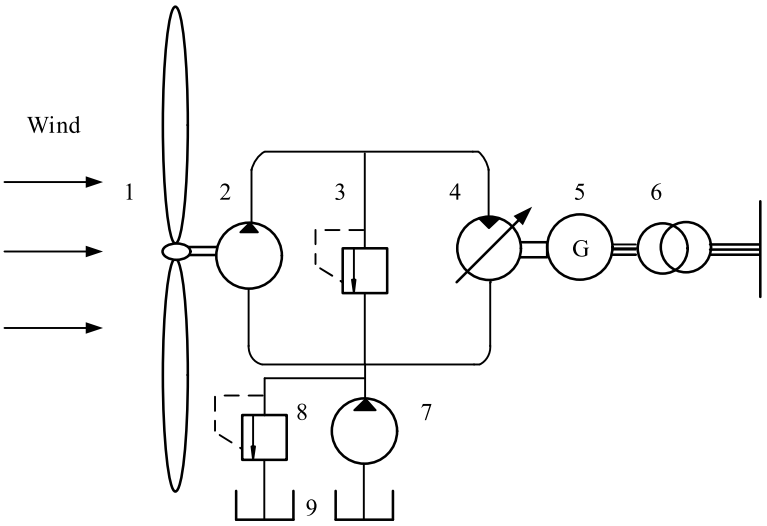

FIGURE 2. Schematic drawing of a hydraulic wind turbine. 1. Rotor 2. Constant displacement pump 3. Safety valve 4. Variable motor 5. Synchronous generator 6.Grid 7. Charge pump 8. Relief valve 9.Tank.

parameter characteristics of the long pipeline is not taken into account.

For the pump-motor hydrostatic transmission system with long pipeline studied in this paper, Nedić *et al.* [17] and Ma *et al.* [18] improved the dynamic response of the system to some extent by using P and PIDD algorithms respectively, but did not achieve active control of pressure pulsation. Laguna found that lowering the volumetric efficiency of the hydraulic motor leads to an additional damping of the pressure fluctuation, however, its influence is minor and unlikely to be advantageous when compared with the power loss [19]. Therefore, it is necessary to find an active control method of pressure pulsation in hydrostatic transmission systems without adding additional devices.

In this paper, the hydraulic system impedance model is established based on electric–hydraulic analogy in Section 2. And in Section 3, the mechanism of pressure resonance in long pipelines is analyzed by establishing the pressure transfer function and solving the resonance condition. Section 4 describes the sensitivity of the resonance frequency to each parameter, and an active control strategy to achieve resonance suppression is proposed by adjusting the motor displacement in real time to make system resonance frequency avoid the excitation frequency. Section 5 introduces the multi-objective genetic algorithm (MOGA) for parameter optimization. Some concluding comments are stated in Section 6.

II. SYSTEM IMPEDANCE MODEL

Fig. 2 shows a schematic of a hydraulic wind turbine, which is mainly composed of rotor, constant displacement pump, variable motor and synchronous generator. After the rotor captures the wind energy, it drives the constant displacement pump to rotate to generate high pressure oil through the drive shaft. The high pressure oil then drives the variable motor to rotate, since the synchronous generator and the variable motor are rigidly connected, the synchronous generator will rotate and generate electricity.

A. ELECTRIC–HYDRAULIC ANALOGY

The principle of electric-hydraulic analogy is to transform the hydraulic system into a circuit system with similar structure and characteristics [20], and has been applied to many research fields, such as microfluidic networks [21], pressure transducer [22], and human artery system [23]. Assume that the flow in the system is laminar which implies the Reynolds number is about 2000 or less, then the flow and pressure in the hydraulic system correspond to the current and voltage in the electric circuit system, similarly, corresponding to resistance, capacitance and inductance in the electric circuit system, there are hydraulic resistance, hydraulic capacitance and hydraulic inductance in the hydraulic system. Table 1 shows the analogy between the electric circuit system and the hydraulic system.

B. SOURCE IMPEDANCE MODEL

The constant displacement pump is the source of the hydrostatic transmission system, and the flow continuity equation is expressed by

$$q_1(t) = D_p\omega_p - C_{tp}p_1(t) - \frac{V_p}{\beta_e}\frac{dp_1(t)}{dt} \tag{1}$$

where q_1 denotes output flow of constant displacement pump, D_p pump displacement, ω_p angular speed, C_{tp} leakage coefficient, p_1 pump outlet pressure, V_p high pressure chamber volume of pump, β_e hydraulic oil bulk modulus.

The left part of (1) is the output flow of constant displacement pump, the right side can be divided into the following

TABLE 1. The analogy between the electric circuit system and the hydraulic system.

Electric Circuit System	Symbol	Hydraulic System	Symbol
Voltage	U	Pressure	P
Current	I	Flow	Q
Resistance	$R = U/I$	Hydraulic Resistance	$R = P/Q$
Capacitance	$C = I/\dot{U}$	Hydraulic Capacitance	$C = Q/\dot{P}$
Inductance	$L = U/\dot{I}$	Hydraulic Inductance	$L = P/\dot{Q}$

three parts. The first part is the theoretical flow produced by the constant displacement pump, which can be seen as a flow source, as shown in (2). The second part is the flow loss due to leakage of the constant displacement pump, which can be expressed by hydraulic resistance, as shown in (3). The third part is the flow loss due to oil compression, which can be expressed by hydraulic capacitance, as shown in (4). And these three parts are in parallel, therefore, the source impedance model of the constant displacement pump is shown in Fig. 3.

$$q_s = D_p\omega_p \tag{2}$$

$$q_2(t) = C_{tp}p_1(t) = p_1(t)/R_p \tag{3}$$

$$q_3(t) = \frac{V_p}{\beta_e}\dot{p}_1(t) = C_p\dot{p}_1(t) \tag{4}$$

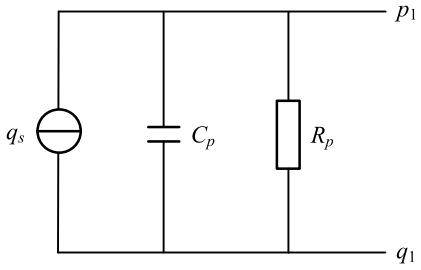

FIGURE 3. Source impedance model.

C. LONG PIPELINE IMPEDANCE MODEL

The fluid transmission pipeline with constant pipeline diameter and axial laminar flow can be described by the transmission line theory (TML). The long pipeline is divided into countless units, each of which is composed of hydraulic resistance R, hydraulic capacity C, and hydraulic inductance L, as shown in Fig. 4.

A pipeline can be represented by the transmission matrix given by [24]

$$\begin{bmatrix} P_1(s) \\ Q_1(s) \end{bmatrix} = \begin{bmatrix} ch\Gamma(s) & Z_C(s)\,sh\Gamma(s) \\ \frac{1}{Z_C(s)}sh\Gamma(s) & ch\Gamma(s) \end{bmatrix} \begin{bmatrix} P_2(s) \\ Q_2(s) \end{bmatrix} \tag{5}$$

where P_1 is the Laplace transformation of pipeline inlet pressure, Q_1 Laplace transformation of pipeline inlet flow, $\Gamma(s) = \chi(s)l$ propagation operator, $\chi(s) = \sqrt{Z(s)Y(s)}$ propagation constant, $Z_C(s) = \sqrt{Z(s)/Y(s)}$ pipeline characteristic impedance, l pipeline length, $Z(s)$ series impedance, $Y(s)$ shunt admittance, P_2 Laplace transformation of pipeline outlet pressure, Q_2 Laplace transformation of pipeline outlet flow.

The pipeline frequency characteristic models mainly include lossless model, linear friction model, and dissipative model [25]. The lossless model does not consider the dissipation and heat transfer effects of the fluid and can easily determine the resonant frequencies of the pipeline. In the linear friction model, the dissipation loss is proportional to the mean flow velocity without considering the heat transfer effect. The dissipation model considers the effects of viscosity and heat transfer simultaneously, but the calculation is complicated. In this paper, we are more concerned about the resonant frequency characteristics of the long pipeline, the linear friction model and dissipative model are too complex to find the exact expression of the resonant frequency. By using the lossless model, we can get the exact expression of the resonant frequency of the system directly and its accuracy is enough. The series impedance, shunt admittance, characteristic impedance, and propagation operator can be described as

$$Z(s) = \frac{\rho}{A}s \tag{6}$$

$$Y(s) = \frac{A}{\rho a^2}s \tag{7}$$

$$Z_C(s) = \sqrt{\frac{Z(s)}{Y(s)}} = \frac{\sqrt{\rho\beta_e}}{A} \tag{8}$$

$$\Gamma(s) = l\sqrt{Z(s)Y(s)} = \frac{l}{a}s \tag{9}$$

where ρ is oil density, $A = \pi d^2/4$ pipeline cross-sectional area, d pipeline diameter, $a = \sqrt{\beta_e/\rho}$ pressure wave propagation speed.

D. TERMINAL IMPEDANCE MODEL

The variable motor and the synchronous generator are the loads of the hydrostatic transmission system. The flow continuity equation and torque balance equation for the variable

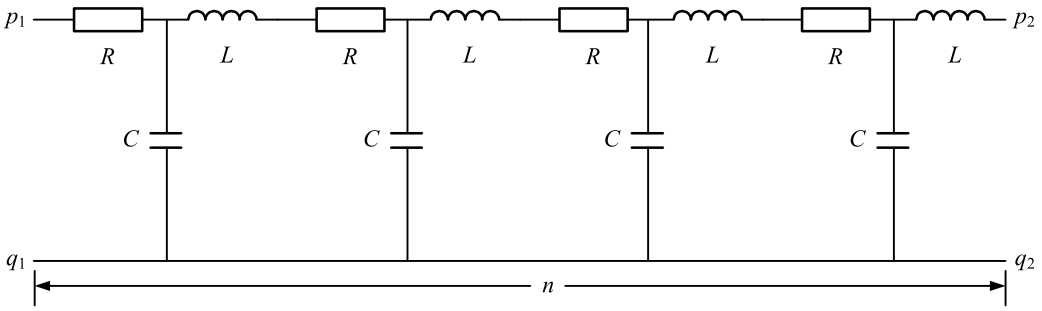

FIGURE 4. Long pipeline impedance model.

motor are respectively established as

$$q_2(t) = D_m\omega_m(t) + C_{tm}p_2(t) + \frac{V_m}{\beta_e}\frac{dp_2(t)}{dt} \tag{10}$$

$$D_m p_2(t) = J_m\frac{d\omega_m(t)}{dt} + B_m\omega_m(t) + T_m \tag{11}$$

where D_m denotes variable motor displacement which is a fixed value when the system works in any stable condition, ω_m rotational speed of variable motor, C_{tm} leakage coefficient, V_m high pressure chamber volume of variable motor, J_m denotes the total inertia of a variable motor and load (converted to the shaft of a variable motor), B_m damping coefficient which is mainly due to the friction caused by the oil film lubrication widely used in hydraulic motors, T_m external load torque acting on the variable motor.

Perform Laplace transformations for (10) and (11), we can obtain

$$Q_2(s) = \frac{D_m^2}{J_m s + B_m}P_2(s) + C_{tm}P_2(s) + \frac{V_m}{\beta_e}sP_2(s) \tag{12}$$

Equation (12) shows that the flow into the variable motor can be divided into the following three parts.

$$Q_{21}(s) = \frac{D_m^2}{J_m s + B_m}P_2(s) \tag{13}$$

$$Q_{22}(s) = C_{tm}P_2(s) \tag{14}$$

$$Q_{23}(s) = \frac{V_m}{\beta_e}sP_2(s) \tag{15}$$

Perform inverse Laplace transformations for (13), (14), and (15).

$$p_2(t) = \frac{J_m}{D_m^2}\dot{q}_{21}(t) + \frac{B_m}{D_m^2}q_{21}(t) = L_m^{'}\dot{q}_{21}(t) + R_m^{'}q_{21}(t) \tag{16}$$

$$p_2(t) = \frac{1}{C_{tm}}q_{22}(t) = R_m q_{22}(t) \tag{17}$$

$$\dot{p}_2(t) = \frac{\beta_e}{V_m}q_{23}(t) = q_{23}(t)/C_m \tag{18}$$

It is easy to know that the above three parts are connected in parallel, and because the motor displacement is adjustable, both L_m' and R_m' are adjustable. Therefore, the variable motor terminal impedance model is shown in Fig. 5.

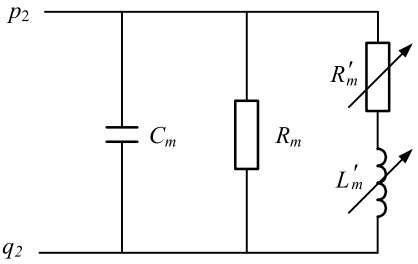

FIGURE 5. Terminal impedance model.

E. SYSTEM OVERALL IMPEDANCE MODEL

Based on the source impedance model, the long pipeline impedance model and the terminal impedance model, the system overall impedance model is established, as shown in Fig. 6. For a long pipeline, its distributed parameter characteristics determine that the system may resonate at multiple frequency points. Even if the amplitude of the pump-side pressure excitation signal is small, a strong pressure pulsation will occur at the variable motor side. Therefore, it is necessary to conduct in-depth research on the resonance mechanism of long pipelines.

III. MECHANISM OF PRESSURE RESONANCE

A. PRESSURE TRANSFER FUNCTION

A pipeline can be represented by the transmission matrix (5), namely,

$$\begin{bmatrix} P_1(s) \\ Q_1(s) \end{bmatrix} = \begin{bmatrix} ch\Gamma(s) & Z_C(s)\,sh\Gamma(s) \\ \dfrac{1}{Z_C(s)}sh\Gamma(s) & ch\Gamma(s) \end{bmatrix} \begin{bmatrix} P_2(s) \\ Q_2(s) \end{bmatrix} \tag{19}$$

It can be rewritten as

$$P_1(s) = P_2(s)ch\Gamma(s) + Q_2 Z_C(s)sh\Gamma(s) \tag{20}$$

So the pressure transfer function of two ends of the long pipeline can be described as

$$G(s) = \frac{P_2(s)}{P_1(s)} = \frac{1}{ch\Gamma(s) + \frac{Z_C(s)}{Z_R(s)}sh\Gamma(s)} \tag{21}$$

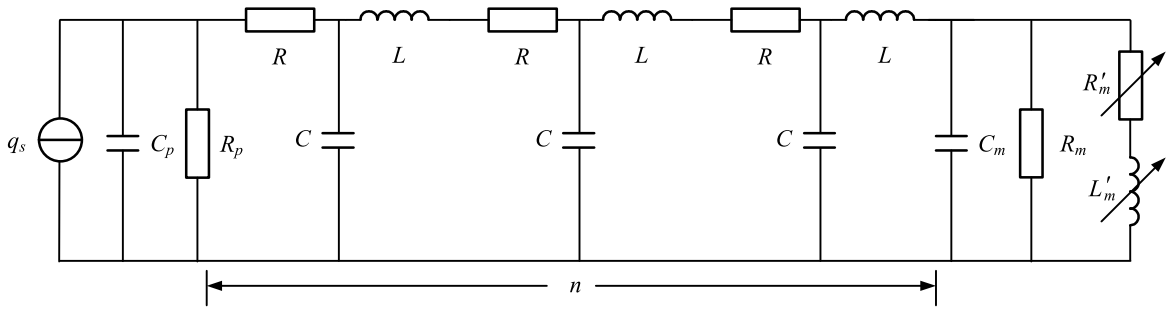

FIGURE 6. System overall impedance model.

where $Z_R(s)$ denotes terminal impedance, ignore variable motor leakage and loss of compression fluid in (12), $Z_R(s)$ is given by

$$Z_R(s) = \frac{P_2(s)}{Q_2(s)} = \frac{J_m s + B_m}{D_m^2} \tag{22}$$

Set $\frac{Z_C(j\omega)}{Z_R(j\omega)} = M + jN$, substitute (8) and (22) into it, M and N are expressed as

$$M = \frac{D_m^2 B_m \sqrt{\rho\beta_e}}{A\left(B_m^2 + J_m^2\omega^2\right)} \tag{23}$$

$$N = -\frac{D_m^2 J_m \omega \sqrt{\rho\beta_e}}{A\left(B_m^2 + J_m^2\omega^2\right)} \tag{24}$$

Substitute (23) and (24) into (21), the pressure frequency characteristic of the long pipeline is given by

$$G(j\omega) = \frac{P_2(j\omega)}{P_1(j\omega)} = \frac{1}{\cos\beta l - N\sin\beta l + jM\sin\beta l} \tag{25}$$

where $\beta = \omega/a$ denotes phase constant.

The pressure amplitude characteristic is expressed as

$$A(\omega) = \frac{1}{\sqrt{(\cos\beta l - N\sin\beta l)^2 + M^2\sin^2\beta l}} \tag{26}$$

The pressure phase characteristic is expressed as

$$\varphi(\omega) = \arctan\left(\frac{-M}{\cos\beta l - N\sin\beta l}\right) \tag{27}$$

B. RESONANCE CONDITION

Resonance happens when the pressure amplitude characteristic shows a maximum value. Solving resonance conditions will lay a theoretical foundation for the formulation of active control strategies for resonance suppression.

To find the maximum value of the pressure amplitude characteristic in (26), set

$$f = (\cos\beta l - N\sin\beta l)^2 + M^2\sin^2\beta l \tag{28}$$

The derivation of (28) is written as

$$f' = \sqrt{(M^2+N^2-1)^2 + 4N^2}\sin(2\beta l + \varphi) \tag{29}$$

where

$$\varphi = \begin{cases} \arctan\dfrac{-2N}{M^2+N^2-1} & M^2+N^2-1 > 0 \\ \arctan\dfrac{-2N}{M^2+N^2-1} + \pi & M^2+N^2-1 < 0. \end{cases}$$

It is easily to know from the sinusoidal function curve, when $2\beta l+\varphi = n\pi, n = 0, 2, 4\cdots, f' = 0$, when $2\beta l+\varphi < n\pi, n = 0, 2, 4\cdots, f' < 0$, and when $2\beta l + \varphi > n\pi, n = 0, 2, 4\cdots, f' > 0$. Therefore, the original function f can get the minimum value when $2\beta l + \varphi = n\pi, n = 0, 2, 4\cdots$. So the condition for resonance in long pipelines is

$$2\beta l + \arctan\frac{-2N}{M^2+N^2-1} \begin{cases} n\pi, n = 0, 2, 4\cdots & M^2+N^2-1 > 0 \\ n\pi, n = 1, 3, 5\cdots & M^2+N^2-1 < 0 \end{cases} \tag{30}$$

C. ANALYSIS OF THE MECHANISM OF PRESSURE RESONANCE

We know that pressure propagates in the pipeline in the form of waves, and the pressure at any point is the superposition of the incident wave and the reflected wave formed by the incident wave arriving at the load. Equation (20) can be written in the following form, where the first term is the incident wave and the second term is the reflected wave.

$$P_1(s) = \frac{1}{2}\left[P_2(s) + Z_C(s)Q_2(s)\right]e^{\gamma(s)l} + \frac{1}{2}\left[P_2(s) - Z_C(s)Q_2(s)\right]e^{-\gamma(s)l} \tag{31}$$

Set reflection constant as

$$\rho_r = \frac{Z_R(s) - Z_C(s)}{Z_R(s) + Z_C(s)} \tag{32}$$

Then equation (31) can be rewritten as

$$\begin{aligned} P_1(s) &= \frac{1}{2}P_2(s)\left[1 + \frac{Z_C(s)}{Z_R(s)}\right]e^{j\beta l} \\ &\quad + \frac{1}{2}\rho_r P_2(s)\left[1 + \frac{Z_C(s)}{Z_R(s)}\right]e^{-j\beta l} \\ &= \frac{1}{2}P_2(s)\sqrt{(1+M)^2+N^2}e^{j(\sigma+\beta l)} \\ &\quad + \frac{1}{2}\rho_r P_2(s)\sqrt{(1+M)^2+N^2}e^{j(\sigma-\beta l)} \end{aligned} \tag{33}$$

where $\sigma = \arctan\frac{N}{1+M}$.

Substitute (8) and (22) into (32), reflection constant can be described as

$$\rho_r = \frac{\sqrt{\left(1-M^2-N^2\right)^2+4N^2}}{(1+M)^2+N^2} e^{-j(\varphi+\pi)} \tag{34}$$

The initial end pressure of the pipeline can be eventually expressed as

$$\begin{aligned} P_1(s) = &\frac{1}{2}P_2(s)\sqrt{(1+M)^2+N^2}e^{j(\sigma+\beta l)} \\ &+\frac{1}{2}P_2(s)\sqrt{(1+M)^2+N^2} \\ &\times \frac{\sqrt{\left(1-M^2-N^2\right)^2+4N^2}}{(1+M)^2+N^2} e^{j(\sigma-\varphi-\beta l-\pi)} \end{aligned} \tag{35}$$

From (35), we can see that compared with the incident wave, the reflected wave not only has an amplitude attenuation with a ratio of $\sqrt{\left(1-M^2-N^2\right)^2+4N^2}/[(1+M)^2+N^2]$, but also a $2\beta l+\varphi+\pi$ delay in phase. The system is in a partially reflective state between no reflection and total reflection. One part of the incident wave energy is absorbed by the terminal load, and the other part is reflected. The transmission line has both traveling wave and standing wave. When the incident wave and the reflected wave are of reverse phase, that is when $2\beta l+\varphi+\pi = n\pi, n = 1,3,5\cdots$, namely, $2\beta l+\varphi = n\pi, n = 0,2,4\cdots$, the amplitude of the superimposed wave of incident wave and reflected wave is the smallest, as shown in Fig. 7, so the correctness of the resonant condition (30) is verified from the perspective of theoretical analysis. The resonance peak is given by

$$A_{\max}(\omega) = \frac{1}{\frac{1}{2}\sqrt{(1+M)^2+N^2}\left[1-\frac{\sqrt{(1-M^2-N^2)^2+4N^2}}{(1+M)^2+N^2}\right]} \tag{36}$$

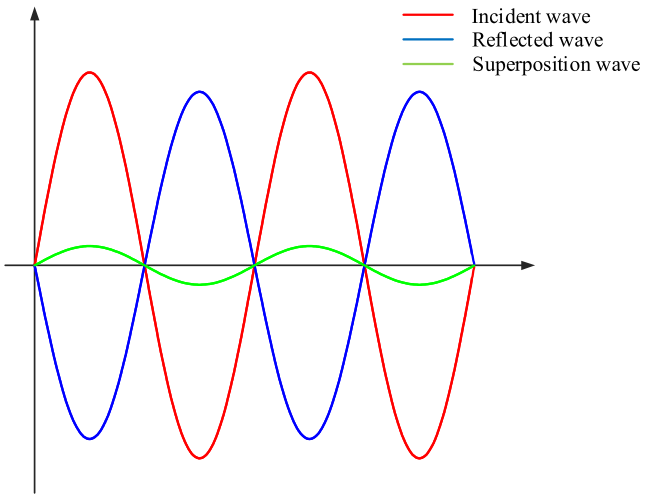

FIGURE 7. Superposition of the incident wave and the reflected wave.

IV. SENSITIVITY ANALYSIS

Sensitivity analysis refers to the analysis of the sensitivity of the system performance due to changes in parameters, and it is an effective means to quantitatively study the influence of system parameters on system performance. The pressure resonance condition (30) contains a plurality of structural parameters and control parameters, in order to clarify the sensitivity of the resonance frequencies to various parameters, as well as provide a theoretical basis for the wind turbine structure design and resonance suppression strategy formulation, the orthogonal test design is carried out based on the Isight software. The design of experiment (DOE) module in Isight is used to design the parameters, and the corresponding orthogonal tables are produced. Each group of parameters in the orthogonal table is calculated by calling the MATLAB program, and the results are transmitted to the Isight for sensitivity analysis.

A. PARAMETER SETTING

For the wind turbines of different power levels, the structure parameters such as pipe length, pipe diameter and moment of inertia are very different. Even for a certain model, the control parameters such as motor displacement are also time-varying under different operating conditions. Table 2 shows the variables and corresponding parameter levels in orthogonal test. Other parameters such as oil density, oil bulk modulus, and damping coefficient are constants. The values of constants are shown in Table 3.

B. MATLAB SOLUTION

From (30), we know that the resonance condition equation is a piecewise function, and sub-domains contains the variable to be solved, namely, the resonance frequency. Fig. 8 is a flow chart for the first solution of the resonant frequency. First, the resonance frequency is solved based on the first

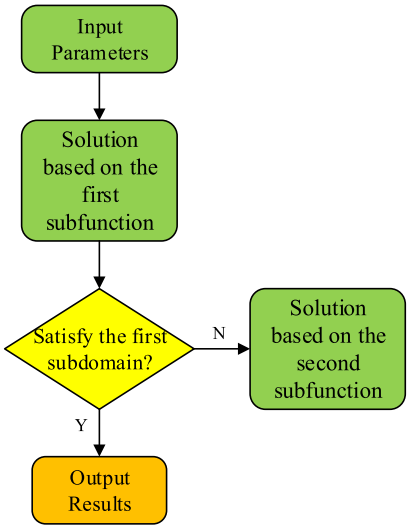

FIGURE 8. Flow chart for the solution of the first resonant frequency.

TABLE 2. Parameter levels of variables.

Symbol	Variable	Level 1	Level 2	Level 3
l	Pipe Length (m)	50	100	150
d	Pipe Diameter (m)	0.016	0.04	0.0825
J_m	Moment of Inertia (kg·m^2)	0.5	10	40
D_m	Motor Displacement (m^3/rad)	9.5×10^{-6}	7.6×10^{-5}	2.30×10^{-4}

TABLE 3. Values of constants.

Symbol	Constant	value
ρ	Oil Density (kg/m^3)	860
B_m	Damping Coefficient (N•m/(rad/s))	0.01
β_e	Oil Bulk Modulus (Pa)	1.7×10^9

subfunction of (30), and then the solution is substituted into the first subdomain to check whether it is satisfied. If it is satisfied, it is the correct solution; otherwise, the resonance frequency is solved based on the second subfunction of (30), and the solution must be the correct solution.

C. RESULT ANALYSIS

Fig. 9 shows the sensitivity analysis results. As we can see, the sensitivity of each variable to the resonant frequency from high to low is: pipe length, variable motor displacement, moment of inertia, pipe diameter. Changing the pipeline length is the most effective way to offset the resonance point, and the motor displacement, moment of inertia, and pipeline diameter will also affect the resonance frequency to some extent.

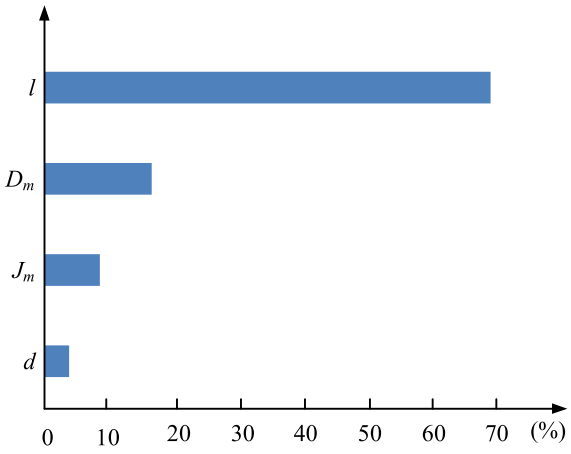

FIGURE 9. Sensitivity analysis results.

Since the excitation of wind turbines is time-varying, the structural parameters such as pipe length, moment of inertia, and pipe diameter cannot be controlled in real time online to make the resonance frequency avoid the excitation frequency, therefore, it is theoretically possible to control the resonant frequency by modifying the displacement of variable motor online.

D. FEASIBILITY ANALYSIS

As we learned in the previous section, it may be feasible to modify the variable motor displacement to achieve resonance suppression. However, there are still two questions to be solved. The first question is that it is still unknown whether other variables, such as pipe length, pipe diameter, and moment of inertia will affect the sensitivity of the variable motor displacement to the resonant frequency, and how much the offset of the resonant frequency will occur when the motor displacement is adjusted. The second question is how the change of variable motor displacement will affect the resonant peak value of pressure.

1) CHANGE LAW OF RESONANT FREQUENCY

Fig. 12, Fig. 13, and Fig. 14 show the variation law of the first resonant frequency when the variable motor displacement and moment of inertia, variable motor displacement and pipeline length, variable motor displacement and pipeline diameter are changed together.

We can see from the figures that the smaller the moment of inertia and the smaller the pipeline diameter, the more sensitive the first resonant frequency is to the variable motor displacement, and the larger the variation range of the first resonance frequency is. That is, the more effective the control strategy of resonance suppression is by adjusting the variable motor displacement. The length of the pipeline will not affect the sensitivity of the first resonance frequency to the variable motor displacement. Higher order resonance frequencies also show the same law as the first order.

Therefore, from the above analysis, we can know that in the design of the wind turbine hydraulic systems, when the power level is determined, the system pressure should be reduced within an appropriate range in order to increase the variable motor displacement. The pipe diameter of the hydraulic long pipeline and the moment of inertia of the variable motor end

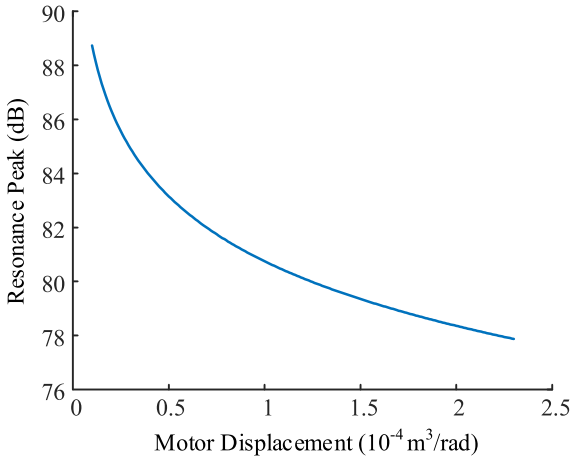

FIGURE 10. Variation of the resonance peak with variable motor displacement.

should be reduced properly so as to better carry out the active control of resonance suppression.

2) CHANGE LAW OF RESONANCE PEAK

Fig. 10 shows the variation of resonant peak with motor displacement.

We can see that the resonance peak decreases with the increase of motor displacement. Therefore, in order to ensure that the pressure fluctuation amplitude after active control is smaller than that before active control, the motor displacement needs to be adjusted to the direction of a greater value in the active control process.

V. CONTROL STRATEGY

In the wind turbine system, due to the randomness of the winds, the excitation frequency of the main drive system is time-varying. The control of the terminal impedance is realized by adjusting the motor displacement in real time, so that the resonant frequency of the hydraulic pipeline in the main system is far away from the resonant frequency, thus reduce the amplitude of the pressure response, as shown in Fig. 11. However, since the rotation speed of the rotors generally works at the maximum power tracking point (MPPT) to capture the most wind energy, adjusting the variable motor displacement will keep the wind turbine away from the MPPT, which will result in the loss of wind energy and the reduction of wind energy utilization efficiency.

Therefore, two optimization objective functions of pressure pulsation attenuation and wind energy loss are established. The MOGA is used to optimize the control of variable motor displacement.

A. PRESSURE PULSATION ATTENUATION OBJECTIVE FUNCTION

Assume that before the resonance suppression is performed, the maximum pulsating pressure peak in the pipeline is G_1, and pulsating pressure amplitude after the resonance suppression control is adopted is G_2, as shown in Fig. 11. The pressure pulsation attenuation is defined as

$$K = 20\lg\left|\frac{G_2}{G_1}\right| \tag{37}$$

Obviously, it is a negative number, and the smaller it is, the better the control effect is. Assume that the variable motor displacement is D_{m0}, the resonance frequency is ω_0 when the system is in resonance, and the motor displacement is D_{m1} after active control. Then G_1 and G_2 can respectively be described as

$$G_1 = \left|\frac{1}{ch\Gamma(j\omega_0) + \frac{Z_C(j\omega_0)}{Z_{R1}(j\omega_0)}sh\Gamma(j\omega_0)}\right| \tag{38}$$

$$G_2 = \left|\frac{1}{ch\Gamma(j\omega_0) + \frac{Z_C(j\omega_0)}{Z_{R2}(j\omega_0)}sh\Gamma(j\omega_0)}\right| \tag{39}$$

where $Z_{R1}(j\omega_0) = \frac{B_m + jJ_m\omega_0}{D_{m0}^2}$, $Z_{R2}(j\omega_0) = \frac{B_m + jJ_m\omega_0}{D_{m1}^2}$.

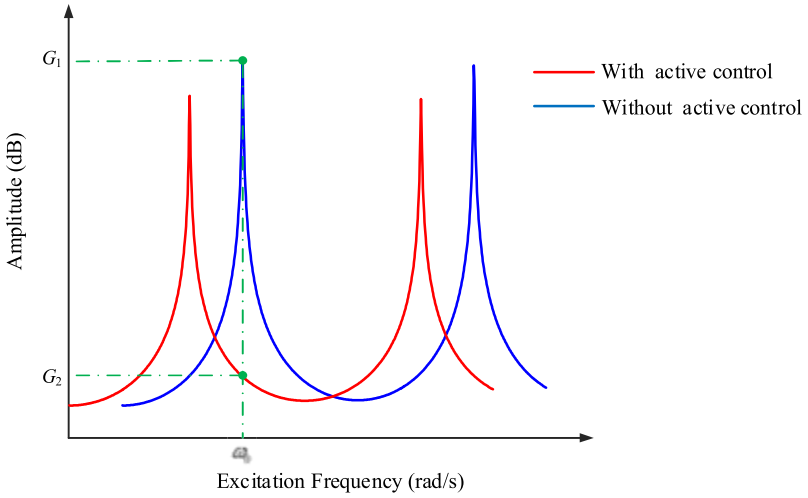

FIGURE 11. Diagrammatic sketch of active control strategy.

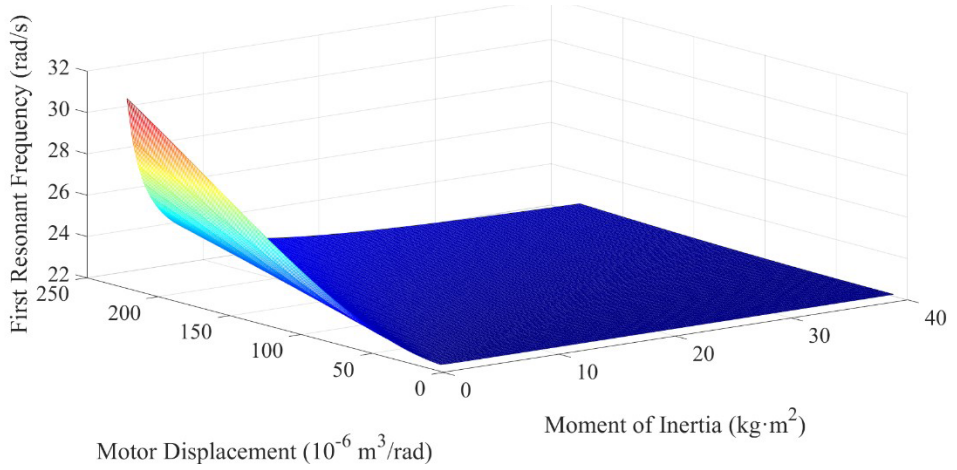

FIGURE 12. Variation of the first resonant frequency with variable motor displacement and moment of inertia.

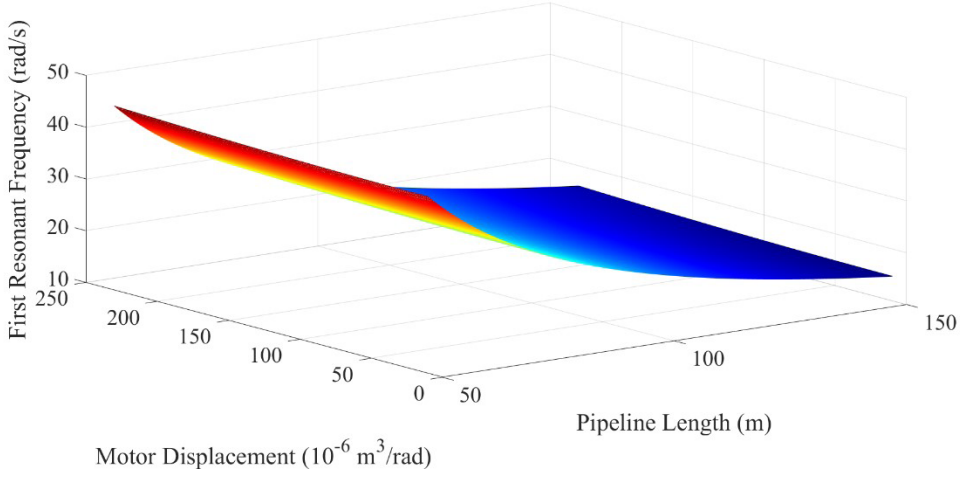

FIGURE 13. Variation of the first resonant frequency with variable motor displacement and pipeline length.

B. WIND ENERGY LOSS OBJECTIVE FUNCTION

The wind energy captured by the rotors is given by

$$P_w(\lambda) = \frac{1}{2}\rho_a \pi R^2 v^3 C_P(\lambda) \tag{40}$$

where $C_P(\lambda)$ denotes the power coefficient, ρ_a the density of air, λ the tip-speed ratio, v the wind speed, R the rotor radius.

The tip-speed ratio λ can be calculated by using the following equation

$$\lambda = \frac{\omega_r R}{v} \tag{41}$$

where ω_r denotes rotor rotational speed.

The power coefficient $C_P(\lambda)$ is given by

$$C_P(\lambda) = C_1\left(\frac{C_2}{\lambda_i} - C_3\right)e^{-\frac{C_4}{\lambda_i}} + C_5\lambda \tag{42}$$

$$\frac{1}{\lambda_i} = \frac{1}{\lambda} + 0.0035 \tag{43}$$

where C_1, C_2, C_3, C_4, C_5 are constants, and their values depend on the shape of the blade.

The wind turbine works at the MPPT before resonance suppression control, at this time $\lambda = \lambda_{\text{opt}}$, wind turbines can catch the most wind energy, which is expressed as

$$P_w(\lambda) = P\left(\lambda_{\text{opt}}\right) \tag{44}$$

When the active control of pressure resonance is performed, the speed of the rotor is given by

$$\omega_{r1} = \frac{n_m D_{m1}}{D_p} \tag{45}$$

The tip-speed ratio is

$$\lambda_1 = \frac{\omega_{r1} R}{v} \tag{46}$$

The wind energy captured by the rotor under this circumstance is given by

$$P_w(\lambda) = P_w(\lambda_1) \tag{47}$$

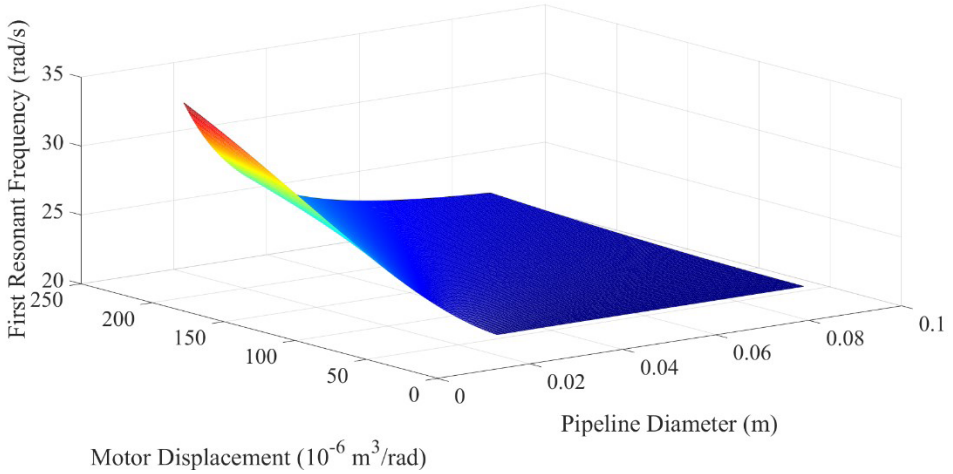

FIGURE 14. Variation of the first resonant frequency with variable motor displacement and pipeline diameter.

TABLE 4. 750 kW bottom founded hydraulic wind turbine technical parameters.

Symbol	Constant	value
P	Rated Power (kW)	750
v	Rated Wind Speed (m/s)	12
ω	Rated Rotational Speed (rad/s)	4.3
R	Rotor Radius (m)	22.4
ρ_a	Air Density (kg/m^3)	1.225
l	Pipeline Length (m)	100
d	Pipeline Diameter (m)	0.0825
J_m	Moment of Inertia (kg·m^2)	40
B_m	Damping Coefficient (N•m/(rad/s))	0.01
β_e	Oil Bulk Modulus (Pa)	1.7×10^{9}
D_m	Motor Maximum Displacement /(m^3/rad)	2.30×10^{-4}
D_p	Pump Displacement (m^3/rad)	8.7×10^{-3}
v_0	Wind Speed at Resonance (m/s)	5.7
D_{m0}	Motor Displacement at Resonance (m^3/rad)	1.15×10^{-4}
λ_{opt}	Optimal Tip Speed Ratio	8
C_1	Blade Shape Parameter	0.5176
C_2	Blade Shape Parameter	116
C_3	Blade Shape Parameter	0.4
C_4	Blade Shape Parameter	5
C_5	Blade Shape Parameter	21

Therefore the wind energy loss objective function can be described as

$$P_{\text{loss}} = P_w\left(\lambda_{\text{opt}}\right) - P_w\left(\lambda_1\right) \tag{48}$$

C. PARAMETER SETTING

This paper takes the 750kW bottom founded hydraulic wind turbine as an example to carry out active control research. The main parameters are shown in Table 4.

In order to prevent excessive wind energy losses in multi-objective optimization, the range of variable motor displacement is given by

$$D_{m1} \in \left[1.15 \times 10^{-4}, 1.5 \times 10^{-4}\right]$$

D. RESULT ANALYSIS

Because the two objectives of the pressure pulsation attenuation and the wind energy loss are mutually restricted, in order to reduce more pressure pulsation, more wind energy utilization efficiency will be lost. The purpose of multi-objective optimization is to find a definite solution in the feasible

domain, so that the conflicting objective functions can reach the extremum at the same time as much as possible.

In this paper, the total number of individuals is 200, the crossover rate is 0.8, the variation rate is 0.2, and the Pareto set is obtained by using the MOGA, after 180 iterations, as shown in Fig. 15.

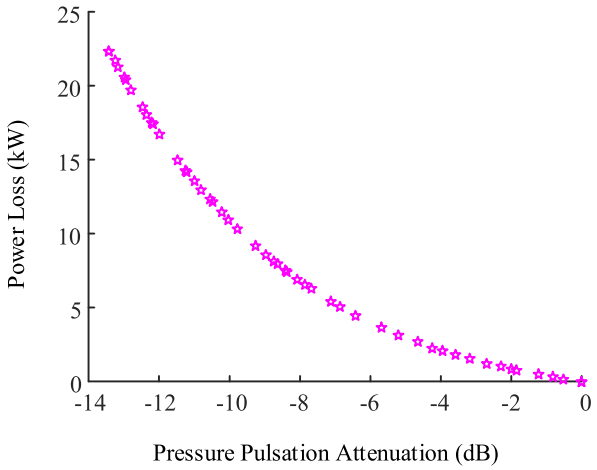

FIGURE 15. Pareto set of pressure pulsation attenuation and power loss taking the variable motor displacement as control object.

TABLE 5. 3 Pareto solutions and corresponding objective function values.

Objective Function Value	Solution 1	Solution 2	Solution 3
Variable Motor Displacement (m^3/rad)	148.6	130.2	121.3
Pressure Pulsation Attenuation (dB)	-13.4	-6.4	-1.87
Wind Energy Loss (kW)	22.3	4.5	0.7

3 Pareto solutions and corresponding objective function values are listed in Table 5. We can see from the table that the resonance suppression control method proposed in this paper can reduce the amplitude of the pressure fluctuation in different degrees which plays a positive role in maintaining the safety of the system and the high quality of electrical energy.

VI. CONCLUSION

(1) Assume that the flow in the system is laminar, the impedance models of the constant displacement pump, the hydraulic long pipeline and the variable motor are established respectively, and the pressure transfer function of two ends of the pipeline is obtained based on the electro-hydraulic analogy theory.

(2) The resonance conditions of the pipeline are obtained by the method of derivation and sensitivity analysis shows that the sensitivity of each variable to the resonant frequency is: pipeline length > variable motor displacement > equivalent rotational inertia > pipeline diameter.

(3) The smaller the equivalent inertia moment and the smaller the pipe diameter are, the more sensitive the resonant frequency is to the variable motor displacement, and the larger the variation range of the resonance frequencies is. The length of the pipeline will not affect the sensitivity of the resonance frequencies to the variable motor displacement.

(4) In order to ensure that the pressure fluctuation amplitude after active control is smaller than that before active control, the motor displacement needs to be adjusted to the direction of a greater value in the active control process.

(5) An active control strategy is proposed to realize resonance suppression by real-time control of motor displacement to change the load impedance so that the system resonance frequencies avoid the excitation frequency.

(6) The pressure pulsation attenuation and wind energy loss objective functions are established respectively. The MOGA is used to optimize the control object, and the attenuation of pressure pulsation amplitude can be achieved in different degrees.

REFERENCES

[1] J. Kersten and H. Aschemann, "LMI approaches for a robust control of a wind turbine with a hydrostatic transmission," in *Proc. IEEE ECC*, Aalborg, Denmark, Jun./Jul. 2016, pp. 1475–1480.

[2] Y. Fan, A. Mu, and T. Ma, "Study on the application of energy storage system in offshore wind turbine with hydraulic transmission," *Energy Convers. Manage.*, vol. 110, pp. 338–346, Feb. 2016.

[3] A. Jarquin-Laguna, "Fluid power network for centralized electricity generation in offshore wind farms," *J. Phys., Conf. Ser.*, vol. 524, no. 1, pp. 1–10, 2014.

[4] D. Buhagiar, T. Sant, and M. Bugeja, "A comparison of two pressure control concepts for hydraulic offshore wind turbines," *J. Dyn. Syst., Meas., Control*, vol. 138, no. 8, p. 081007, Aug. 2016.

[5] H. Schulte and E. Gauterin, "Fault-tolerant control of wind turbines with hydrostatic transmission using Takagi–Sugeno and sliding mode techniques," *Annu. Rev. Control*, vol. 40, pp. 82–92, Dec. 2015.

[6] A. J. Laguna, "Modeling and analysis of an offshore wind turbine with fluid power transmission for centralized electricity generation," *J. Comput. Nonlinear Dyn.*, vol. 10, no. 4, p. 041002, Jul. 2015.

[7] P.-X. Gao, J.-Y. Zhai, Y.-Y. Yan, Q.-K. Han, F.-Z. Qu, and X.-H. Chen, "A model reduction approach for the vibration analysis of hydraulic pipeline system in aircraft," *Aerosp. Sci. Technol.*, vol. 49, pp. 144–153, Feb. 2016.

[8] P. Ouyang, Z. Jiao, H. Liu, S. Li, and Y. Li, "Active control on fluid borne pulsation using piezoelectric valve as absorber," in *Proc. IEEE Conf. Robot. Autom. Mechatronics*, Bangkok, Thailand, Jun. 2006, pp. 686–690.

[9] C. Guan, Z. Jiao, S. Wu, Y. Shang, and F. Zheng, "Active control of fluid pressure pulsation in hydraulic pipe system by bilateral-overflow of piezoelectric direct-drive slide valve," *J. Dyn. Syst., Meas., Control*, vol. 136, no. 3, p. 031025, Mar. 2014.

[10] H. Zheng, Z. Jiao, Y. Xu, and L. Chai, "Efficient active control of fluid borne pulsation in hydraulic piping systems," in *Proc. IEEE Int. Conf. Aircr. Utility Syst. (AUS)*, Beijing, China, Oct. 2016, pp. 1106–1110.

[11] M. Pan, A. Hillis, and N. Johnston, "Active control of fluid-bome noise in hydraulic systems using in-series and by-pass structures," in *Proc. UKACC Int. Conf. Control*, Loughborough, U.K., Jul. 2014, pp. 355–360.

[12] M. Pan, N. Johnston, and A. J. Hillis, "Active control of pressure pulsation in a switched inertance hydraulic system using a rectangular-wave reference signal," in *Proc. ASME/BATH FPMC*, Bath, U.K., 2013, pp. 610–620.

[13] J. Cheer and S. Daley, "Broadband active control of noise and vibration in a fluid-filled pipeline using an array of non-intrusive structural actuators," in *Proc. 44th Int. Congr. Noise Control Eng.*, San Francisco, CA, USA, 2015, pp. 3492–3501.

[14] M. J. Brennan, S. J. Elliott, and R. J. Pinnington, "A non-intrusive fluid-wave actuator and sensor pair for the active control of fluid-borne vibrations in a pipe," *Smart Mater. Struct.*, vol. 5, no. 3, pp. 281–296, 1996.
[15] E. Kojima, M. Shinada, and T. Yamaoka, "Development of an active attenuator for pressure pulsation in liquid piping systems: 2nd report, trial construction of the system and fundamental experiments of attenuation characteristics," *Trans. Jpn. Soc. Mech. Eng. Ser. B*, vol. 57, no. 541, pp. 2984–2991, 1996.
[16] E. Kojima, M. Shinada, and M. Shinbo, "Development of an active attenuator for pressure pulsation in liquid piping systems: 1st report, a real time-measuring method of progressive wave in a pipe," *JSME Int. J. Ser. B*, vol. 56, no. 530, pp. 2937–2944, 1990.
[17] N. N. Nedić, V. Filipović, and L. M. Dubonjić, "Design of controllers with fixed order for hydraulic control system with a long transmission line," *FME Trans.*, vol. 38, no. 2, pp. 79–86, 2010.
[18] Q. Ma *et al.*, "Research on feed-forward PIDD2 control for hydraulic continuous rotation motor electro-hydraulic servo system with long pipeline," presented at the UKACC 11th Int. Conf. Control, Belfast, U.K., Aug./Sep. 2016.
[19] A. J. Laguna, N. F. Diepeveen, and J. W. Van Wingerden, "Analysis of dynamics of fluid power drive-trains for variable speed wind turbines: Parameter study," *IET Renew. Power Generat.*, vol. 8, no. 4, pp. 398–410, 2014.
[20] J. C. Schönfeld, "Analogy of hydraulic, mechanical, acoustic and electric systems," *Appl. Sci. Res., Sect. A*, vol. 3, no. 1, pp. 417–450, 1954.
[21] K. W. Oh, K. Lee, B. Ahn, and E. P. Furlani, "Design of pressure-driven microfluidic networks using electric circuit analogy," *Lab Chip*, vol. 12, no. 3, pp. 515–545, 2012.
[22] C. Clark, "A differential pressure transducer for the measurement of high-frequency fluctuations in liquids," *J. Phys. E, Sci. Instrum.*, vol. 18, no. 4, pp. 297–302, 1985.
[23] A. Quarteroni, S. Ragni, and A. Veneziani, "Coupling between lumped and distributed models for blood flow problems," *Comput. Vis. Sci.*, vol. 4, no. 2, pp. 111–124, 2001.
[24] N. Johnston, "The transmission line method for modelling laminar flow of liquid in pipelines," *Proc. Inst. Mech. Eng., I, J. Syst. Control Eng.*, vol. 226, no. 5, pp. 586–597, 2012.
[25] S. Chakraborty and R. Chowdhury, "A hybrid approach for global sensitivity analysis," *Rel. Eng. Syst. Saf.*, vol. 158, pp. 50–57, Feb. 2017.

CHAO AI was born in Tangshan, China, in 1982. He received the B.S., M.S., and Ph.D. degrees in mechanical engineering from Yanshan University, Qinhuangdao, China, in 2005, 2008, and 2012, respevtively.

From 2013 to 2015, he was a Lecturer with the Mechanical Engineering Department, Yanshan University, where he is currently an Assistant Professor. His research interests include hydraulic wind turbines, hydraulic component optimization design, and hydraulic servo systems. He has published over 20 academic pepers and participated in over 10 national research projects.

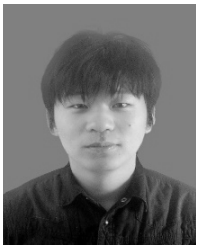

WENJIE BAI was born in Handan, China, in 1994. He received the B.S. degree in mechanical engineering from Yanshan University, Qinhuangdao, China, in 2016, where he is currently pursuing the M.S. degree in mechanical engineering.

His areas of research include hydraulic wind turbine control theory, fluid dynamics, hydraulic system design, and pipeline vibration dynamics.

TINGYUAN ZHANG was born in Cangzhou, China, in 1995. He received the B.S. degree in mechanical engineering from Yanshan University, Qinhuangdao, China, in 2017, where he is currently pursuing the M.S. degree in mechanical engineering.

His research interest includes the study of hydraulic wind turbine control theory, pipeline resonance suppression, and fluid fluctuation reduction.

XIANGDONG KONG received the B.S. degree in mechanical engineering from Zhejiang University, Hangzhou, Zhejiang, China, in 1982, and the M.S. and Ph.D. degrees from Yanshan University, Qinhuangdao, China, in 1985 and 1991, respectively.

Since 1996, he has been a Professor with the Mechanical Engineering Department, Yanshan University. From 2001 to 2001, he was a Senior Visiting Scholar with the University of Illinois at Urbana–Champaign. He has authored five books and over 180 academic papers, and holds 14 patents. His research interests include electro-hydraulic servo control system, fluid power transmission and control for heavy machinery, high performance hydraulic components, vibration control on hydraulic system, and digital hydraulic technology.

Prof. Kong is a board member of Chinese Mechanical Engineering Society and also a President of the Hebei Province Mechanical Engineering Society.